

# **Diving in exoplanets: are water seas the most common?**

**F. J. Ballesteros<sup>1,\*</sup>, A. Fernandez-Soto<sup>2,3</sup>, and V. J. Martínez<sup>1,3,4</sup>**

<sup>1</sup> Observatori Astronòmic, Universitat de València, C/ Catedrático José Beltrán 2, E46980-Paterna (València), Spain.

<sup>2</sup> Instituto de Física de Cantabria (CSIC-UC), E39005-Santander, Spain.

<sup>3</sup> Unidad Asociada Observatori Astronòmic (IFCA-UV), E46980-Valencia, Spain.

<sup>4</sup> Departament d'Astronomia i Astrofísica, Universitat de València, E46100-Burjassot (València), Spain

\* fernando.ballesteros@uv.es, phone: +34 96354 3746, fax: +34 96354 3744.

## **ABSTRACT**

One of the basic tenets of exobiology is the need for a liquid substratum in which life could arise, evolve and develop. The most usual version of this idea involves the necessity of water to act as such a substratum, both because that is the case on Earth and because it seems to be the most viable liquid for the chemical reactions leading to life. Other liquid media that could harbour life have, however, been

occasionally put forth. In this work we investigate the relative probability of finding superficial seas on rocky worlds that could be composed of nine different, potentially abundant liquids, including water. We study the phase space size of habitable zones defined for those substances. The regions where they can be liquid around every type of star are calculated using a simple model, excluding areas within a tidal locking distance. We combine the size of these regions with the stellar abundances in the Milky Way disk, and modulate our result with the expected radial abundance of planets via a generalized Titius-Bode law, as statistics of exoplanet orbits seem to point to its adequateness. We conclude that seas of ethane may be up to nine times more frequent among exoplanets than seas of water, and that solvents other than water may play a significant role in the search for extrasolar seas.

Keywords: exoplanets - habitable zone - exoseas.

## 1 Introduction

The aim of this paper is to face the following question: Which solvent could in principle be most frequent for sustaining life? Implicitly this question is addressing some basic concepts: How liveable is the circumstellar habitable zone? How frequent are non-water seas in the Universe? Are there other solvents which could have harboured the origins of life on their home planet and hence became the staple liquid for their internal chemical reactions? In other words, how likely would alien biological machinery to be based on water?

The feasibility of other solvents for life has been often considered by many authors (Bains 2004, Benner *et al.* 2004, National Research Council 2007, Stevenson *et al.* 2015) with very suggestive outcomes, as the high viability of organic chemistry in hydrocarbon solvents, the possibility of membrane alternatives in nonpolar solvents, or even the feasibility of complex non-carbon chemistry. Although given the nature of the subject some results are debated, the main conclusion in all these investigations is that it is not possible to discard the possibility of life appearing in solvents other than water.

In this work we will not deal with the possible efficiency, adequateness, or even feasibility of the different solvents to host the earliest reactions driving to the origin of life in different planets. We will just look at the background conditions that eventually can allow the existence of rocky worlds with seas of the

substances considered. We assume that the actual presence of worlds with seas in the Galaxy mimics the abundance of these background conditions. In short, we will try to estimate the relative cosmic abundance of non-water seas in the Universe by measuring their phase space volume; thus, the higher the number of *a priori* configurations that may allow marine worlds of a given substance, the higher the number of worlds that could actually develop such seas. Our work is inspired by previous works such as Bains (2004), but take into account effects as the radial distribution of planetary orbits estimated from exoplanetary data, and the effect of tidal locking on planets close to their parent star. We will try to avoid features that depend on particular planets, therefore necessarily assuming some simplifications. We will assume a uniform temperature distribution (i.e. rapidly rotating worlds) outside the tidal locking region but not inside it, although we will also study the effect of relaxing this condition, obtaining similar results. We will also consider that these solvents have long term stability, not taking directly into account peculiarities of specific unknown planets as atmospheric gas escape or photolysis due to ultraviolet star radiation. Nevertheless, as we will argue in the discussion, photolysis could play a not so relevant role. Given the robustness of our results, even with those caveats we think that our results can cast some light in the programs searching for habitable planets, nowadays focused on the “follow the water” canonical strategy.

This manuscript is organized as follows: In Section 2 we will choose, present,

and characterize a series of chemical compounds that have been suggested as possible environments for life-like reactions; define a simple, generalized habitable zone for each potential liquid candidate and apply a simple correction for atmospheric effects, and compare the result of our assumptions with the most widely studied case: habitable zones defined for water. In Section 3 we present a generalized model of the Titius-Bode law, that will allow us to estimate the radial distribution of orbiting planets with respect to their parent stars, and fit this model to real exoplanetary data in order to have a realistic global orbital distribution of planets. We also discuss the importance of the rocky vs giant gas planet dichotomy for our study. Section 4 presents a brief discussion of the tidal locking effect, and how it would affect our calculations. We introduce in Section 5 a compilation of data on main sequence stars in our Galaxy and their basic properties, that will be necessary to perform our analysis. Finally, in Section 6 we combine all the previous data to obtain an estimate of the relative frequency of rocky worlds that could have surface seas of different substances and discuss these results. We present our conclusions in Section 7.

## **2 Alternatives to water in the Universe and generalized habitable zones**

The list of candidate substances that could exist in liquid form on some particular world could in principle be overwhelming. In order to limit the scope of this work we will consider those liquids that have been proposed in the literature as water

alternatives for life (see for example Bains 2004, Benner *et al.* 2004, National Research Council 2007, Tinetti 2010) and have also been positively detected in exoplanetary atmospheres and in Solar System bodies via spectroscopy (Lodders 2003, Encrenaz *et al.* 2005, Swain *et al.* 2009, Bean *et al.* 2010). Not surprisingly, these relatively abundant substances are the simplest compounds of the most abundant elements of the Universe (i.e. CHONS): water ( $\text{H}_2\text{O}$ ), methane ( $\text{CH}_4$ ), ethane ( $\text{C}_2\text{H}_6$ ), molecular nitrogen ( $\text{N}_2$ ), ammonia ( $\text{NH}_3$ ), sulfuric acid ( $\text{H}_2\text{SO}_4$ ), hydrogen sulfide ( $\text{H}_2\text{S}$ ), carbon dioxide ( $\text{CO}_2$ ) and hydrogen cyanide ( $\text{HCN}$ ). We do not include molecular Hydrogen ( $\text{H}_2$ ) in the analysis presented here since it has never been suggested as a possible substrate for life and hardly anything except helium and neon could be soluble in it; besides, given its extremely low melting and boiling points (14 to 20 K at 1 atm.) it would be hard to find a planet cold enough with an atmosphere dense enough to maintain it liquid (nevertheless we did in fact apply our technique to it, as discussed in Section 6). Table 1 lists pressure and temperature for the triple and critical points for these substances, together with a graphical representation of their liquid phase on a pressure-temperature diagram.

We do not attempt to estimate the *a priori* abundance of each of these chemical species, because the phenomena associated to the planet/satellite/atmosphere formation and evolution processes lead to very complex situations, as we can witness in our own Solar System. We only assume

that the quantity of each of these substances in any given planet is enough to form seas under favorable conditions. We contend that, for example, doubling the original abundance of water in the gas cloud that gave rise to the Solar System would very probably cause the Earth oceans to be deeper and/or to cover a larger fraction of the planetary surface. We would not, however, expect the effects of such a change to include the generation of water oceans on a second planet in our System, as the main limiting condition is the presence of only one world well within the water-defined circumstellar habitable zone. We thus assume that beyond a given minimum threshold the abundances do not modulate our results on the number of potential seas, only their putative sizes or depths. Notice that in this context we use the word “seas” to mean “substantial and enduring bodies of liquid on the surface of a rocky world”. In the case of the Solar System, to which we will often turn to for obvious reasons, these would include both seas and lakes on Earth, and *maria* and *lacūs* on Titan.

The circumstellar habitable zone (Doyle 1996) could be naïvely defined as the region around a star where liquid water can be expected, taking into consideration stellar irradiation as the only energy source. Similar considerations could be done for other solvents. We want to explore and compare the available phase space volume for each of the considered liquids, which will be representative of their probability of presence. In order to reach this objective, we will use a simple base model where irradiation by the central star is the only factor taken into account,

other than the stellar and orbital properties. We then modify this base model by allowing for the counteracting effects of planetary albedo and atmospheric absorption (greenhouse effect) through a simple approximation. We do not consider the possible effect of internal heating, which could be important for young planetary systems or moons in close orbits around massive planets.

## 2.1 The basic temperature model

Within our simple, basic model, we consider that stellar emission can be approximated to that of a black body, thus using Stephan-Boltzmann's law the emission of the star will be  $L = \sigma T_*^4 4\pi R_*^2$ , where  $R_*$  is the radius of the star and  $T_*$  its surface temperature. Suppose a planet at a distance  $a$  from the star. The power received per unit area decreases with the distance squared according to  $P = L/4\pi a^2$ . For the entire planet, the total power received will be  $E_{in} = \pi R_p^2 P$ , where  $R_p$  is the radius of the planet. This power will be in equilibrium with the thermal power radiated by the planet,  $E_{out} = \sigma T_{eq}^4 4\pi R_p^2$  where  $T_{eq}$  is the equilibrium temperature of the planet for zero albedos. Equating  $E_{in}$  and  $E_{out}$  we obtain:

$$a = \frac{1}{2} R_* (T_* / T_{eq})^2. \quad (1)$$

Knowing the temperature and radius of the star and substituting  $T_{eq}$  by the values of melting and boiling temperatures of water, we obtain the distances to the star  $a_{melting}$  and  $a_{boiling}$  that limit the (water) habitable zone. To extend this definition to other liquids, just substitute in Eq. 1  $T_{eq}$  by the melting and boiling



temperatures for the liquid under consideration, thus obtaining an analogously defined “circumstellar habitable zone” for methane, ammonia, etc.

Note that the boiling and melting temperatures depend on pressure, and in principle we do not know the surface atmospheric pressure of unknown exoplanets. Therefore, in order to be able to perform a comparison among liquids, we will consider 43 atmospheric pressures distributed from  $10^{-8}$  to 316 atm, averaging afterwards the results using a logarithmic equal-weight scheme, as surface pressures in several Solar System’s rocky bodies distribute more uniformly under a logarithmic representation (see ticks in the right margin of the diagram in Table 1). This range is enough to include pressures between the critical and triple points for each of our substances, as seen in Table 1. As an example, we show in Figure 1 how the liquid phase regions in the phase diagram translate into distances via Equation 1 around a star for three different stellar types. Notice that under this logarithmic representation the shape and size of the different regions do not change, but move towards or away from the star as a function of its temperature. This stems from the fact that, in equation 1,  $T_*^2$  is a multiplicative factor that in logarithmic space translates into an additive factor which just shifts the regions. Notice also that although in the phase diagram the available phase space of liquid water is comparable to that of liquid ethane, it gets considerably smaller when represented in this way.

## 2.2 A simple albedo and greenhouse model

We will not attempt a full modelization of the effects of albedo and greenhouse gases on the atmospheres of planets with different atmospheric compositions. We consider that such an analysis would be beyond the scope of this paper, and it may in fact be very difficult to compile all the necessary data for it. As a comparison, detailed atmospheric models exist for the greenhouse (and anti-greenhouse) effect on Titan, the Earth, Venus, Mars (Pollack 1979, Kasting 1988, McKay *et al.* 1991, Leconte *et al.* 2013a); other stellar systems (Selsis *et al.* 2007); and even for potential free-floating planets (Badescu 2010a).

Some facts point to the possibility of atmospheric effects in other solvents being less complex than in the case of water. For example, water is unique in our list in having a floating ice, as all the other substances in our list present the usual evolution of density with temperature that makes the solid phase sink. Water vapour presents absorption in spectral bands that match the infrared peak at the atmospheric temperatures of interest, whereas the absorption properties of other substances vary widely (see, for example, Badescu 2010b). While we have not analysed all the solvents in detail, probably the situation in those cases is less complex.

In order to have at least some grasp of the possible influence of greenhouse effect and albedo in our analysis we decided to adopt a simple, coarse-grain model for both of them. First, we approximate the net effect of albedo by

including a factor  $A$  ( $0 \leq A \leq 1$ ) that accounts for the amount of stellar power that gets reflected and does not heat the planet surface. This is similar to the Bond albedo, although we do not intend to use its strict definition. Typical values of the Bond albedo for solar system objects range from  $\sim 0.1$  for dark, rocky objects like Mercury and the Moon, to  $\sim 0.9$  for bright objects like Eris and Venus; with intermediate objects like the Earth, Mars and the giant planets being in the 0.25-0.35 range.

Second, we do also approximate a putative greenhouse effect by correcting the planetary energy output at equilibrium with a factor  $(1 - g)$ , which represents the amount of infrared energy that should be thermally radiated away from the planet but gets trapped by gases in the atmosphere. The magnitude  $g$  stands for the normalized greenhouse effect (Raval & Ramanathan 1989), defined as  $g = G / (\sigma T_s^2)$ , with  $G$  the greenhouse effect or forcing (measured in  $W/m^2$ ). It fulfills  $g = 1 - (T_{eq}/T_s)^2$  where  $T_{eq}$  is the temperature the planetary surface would have with no greenhouse effect and  $T_s$  the temperature it really has. We remark that a completely opaque atmosphere ( $g = 1$ ) would imply that all the energy would be trapped in the planet, leading to a divergence in the equilibrium temperature.

When these two factors are taken into account, the distance  $a$  at which the equilibrium temperature  $T$  is reached is given by

$$a = \frac{1}{2} R_* (T_* / T)^2 \sqrt{\frac{1 - A}{1 - g}}. \quad (2)$$

Our model defines “habitable zones” in a manner which is simple but operational. The liquid water habitable zone in the Solar System that we obtain using the simple base calculation detailed above corresponds to 0.20-1.03 au, which is restricted to 0.54-1.03 au for atmospheric pressures of 1 atm. Allowing for an albedo as large as  $A = 0.5$  the inner border starts at 0.14 au (0.39 au for the case of 1 atm), and allowing for a greenhouse effect as large as  $g = 0.5$  makes the outer border reach to 1.45 au (which is independent of atmospheric pressure in our model). Using more detailed models that include greenhouse effect, albedo and varied atmospheric conditions, including compositions and atmospheric pressures as diverse as present-day Venus, Earth and Mars (Kasting *et al.* 1993, Kopparapu 2013, Kopparapu *et al.* 2013, Vladilo *et al.* 2013) other authors obtain inner radii within the range 0.7-1.0 au, and outer radii within 1.1-1.8 au, with widths of the circumstellar habitable zone ranging between 0.3 and 0.7 au. The very complete model presented by Zsom *et al.* (2013) allows for inner radii of the water habitable zone in the Solar System as small as 0.38 au for high-albedo, low-humidity planets. The habitable zones defined by means of the mentioned detailed models are generally comparable, although in average further away from the Sun than ours.

We treat both the albedo and greenhouse effect so that they affect the habitable zones for the different substances in the same way. Again, both  $\sqrt{1 - A}$

and  $1/\sqrt{1-g}$  are multiplicative factors in equation 2 that in logarithmic space act as additive factors, shifting the regions without any change of size or shape. Black lines in figure 1 show the shift of these regions when considering an albedo of  $A = 0.5$  and no greenhouse effect (dashed lines), and a normalized greenhouse effect of  $g = 0.5$  and no albedo (dotted lines).

On the whole, the wider the circumstellar habitable zone of a given substance, the easier to find a planet inside it would be. Thus, as a first approximation one could consider that the probability to find seas of a given substance will be related to the width of its circumstellar habitable zone, i.e. the value  $a_{melting} - a_{boiling}$ , but there are other factors to take into consideration.

### 3 Radial distribution of planets and the universality of Titius-Bode law

In our Solar System planets are more abundant close to the Sun, whereas planet orbits become more and more widely spaced as we move outwards. This trend is captured by the Titius-Bode law (Nieto 1972) which hypothesizes an exponential radii growth for consecutive orbits, whose only exception is Neptune. A generalized form of this law, known as Dermott's law, has been widely used in the literature (Goldreich & Sciama 1965, Dermott 1968, Lovis *et al.* 2011, Lara *et al.* 2012, Bovaird & Lineweaver 2013) and is given by:

$$a_n = a_0 C^n, \tag{3}$$

where  $a_0$  is the orbital semi-major axis of the innermost planet,  $n = 0, 1, 2, \dots$  is a label indexing the consecutive planets, and  $C$  is a growth factor between consecutive orbits. Applying this version of the law to the Solar System gives  $C \sim 1.9$ . Similar laws have been found with slightly different growth factors in the satellites of several planets:  $C = 2.03$  for Jupiter,  $C = 1.59$  for Saturn and  $C = 1.8$  for Uranus. Therefore in the Solar System a fixed range of distances  $\Delta a = a_{\text{melting}} - a_{\text{boiling}}$  will have higher likelihood to encompass one or several planets if it is close to the Sun. Should we expect a similar behavior in other planetary systems?

As the number of known exoplanets has grown, and more multi-planetary systems have been discovered, several recent works have tried to study whether a similar law is upheld. The outcome of these studies seems to confirm the validity of Dermott's law in several alien planetary systems, see for example Lovis *et al.* (2011), Lara *et al.* (2012), and Huang & Bakos (2014); and especially Bovaird & Lineweaver (2013), where the authors predicted the existence of five planets that were eventually found. The recently found TRAPPIST-1 planetary system also fulfills this law (Gillon *et al.* 2017). Nevertheless the possible universality of this law or whether it is no more than a simple coincidence is still a matter of debate (Kotliarov 2008, Bleech 2014).

In this work we are going to present an alternative, brute force test in order to assess the universality of the Titius-Bode/Dermott's law. Figure 2 shows an histogram of the growth factors that we have extracted from different multi-planet

systems in Lovis *et al.* (2011), Lara *et al.* (2012), Bovaird & Lineweaver (2013), and Gillon *et al.* (2017), together with a fit to a log-normal probability distribution function. We have generated one hundred thousand random planetary systems according to equation 3, with random values for  $a_0$  chosen uniformly between 0.005 and 0.15 au, and random values for  $C$  generated according to the log-normal distribution of Figure 2 (only using values higher than 1). We calculated the histogram of the length of the semi-major axis for planets in all these systems (a total number of  $\sim 900000$  planets in 100000 planetary systems), and the result is shown in Figure 3 (red dots). As can be seen the histogram fits extraordinarily well a power law with exponent  $-1$ , except in the region under 0.15 au due to border effects. Such a result was expected, as an exponential growth in radii corresponds to a uniform distribution in a logarithmic scale—a result we find is independent of the distribution used for the random generation of the  $C$  values.

Assuming that planets were detected via the transit method, not the whole set of generated planets should be expected to be observable from Earth. In fact the probability of observation depends on the orbital inclination, but also on the distance to the central star: if  $R_*$  is the diameter of the star, and  $a$  is the distance of the planet to its star, a given planet would be detectable via the transit method only if the orbital inclination  $\alpha$  were smaller than  $\arctan(R_*/a)$ . Thus the probability of observation will be proportional to  $p(a) \propto \frac{\arctan(R_*/a)}{\pi} \approx \frac{R_*}{\pi} a^{-1}$ ,

which introduces an additional  $a^{-1}$  factor in the power law.

Including this geometrical correction into our model and taking for simplicity  $R_*$  equal to one solar radius (as an average representative value), we obtain the distance distribution for the fraction of planets from our model that we could expect to observe via the transit method (see Figure 3, green dots), following now a power law with exponent  $-2$ . This distribution is to be compared with the black dots in the same figure, which correspond to the orbital semi-major axis histogram for all the real exoplanets detected via the transit method, as listed in the exoplanets.org database. The experimental result is remarkably similar to the outcome of our simple numeric exercise. The main difference is the apparent decrease of detected planets at distances beyond 1 au. Do note, however, that these distances correspond to longer orbital periods, which renders planets at those distances more difficult to detect, an effect not included in our straightforward model.

This result seems to confirm that exoplanetary systems conform reasonably well to a Titius-Bode/Dermotts' law. At least, the probability of the presence of a planet around a star at a given distance  $a$  is approximately proportional to  $a^{-1}$ , which is the result that we will use in our calculations.

### **3.1 The rocky/giant planet dichotomy**

Our definition of “sea” implies the need for a solid surface over which such seas



can extend. It is obvious that in the case of gaseous, giant planets, no such surface is available, but this fact must be combined with the evidence that, in the Solar System, all giant planets (with the possible exception of Uranus) have at least one rocky moon with a size and composition that allows us to include it in our category of worlds that could potentially harbour “substantial and enduring bodies of liquid” on their surface. As a matter of fact the only other world (outside the Earth) where such seas have been detected is Saturn’s moon Titan. Jupiter’s moon Ganymede and Titan itself are larger than Mercury, while Callisto, Io, the Earth’s Moon, Europa and Neptune’s Triton are larger than any of the Solar System dwarf planets. Titan is the only one among them that maintains a dense atmosphere, necessary to support a large liquid surface body. However, giant planet moons do not seem to be different from rocky planets in this respect.

We will use this observation to define an operational conjecture: we will include in our analysis one rocky world, potentially able to accomodate a surface sea, for every orbital distance as given by our numeric Titius-Bode/Dermotts’ Law model.

### **3.2 Orbital parameter dependence on stellar type**

There have been studies on the correlation between stellar spectral types and

planet orbital parameters (see for example Buchhave *et al.* 2014 and Winn & Fabrycky 2015) pointing to planetary systems around M-type stars being more compact and containing smaller fractions of gas giants. These effects could potentially bias our calculations, although the result from our simple simulation (Figure 3, green dots) and the real statistics (same figure, black dots) seem to agree reasonably well. We should in any case remark that it is still difficult to estimate the degree of compactness and the orbital distribution of planets because of the large and non-identical selection effects induced by the two most usual planet detection techniques (Doppler and transit). This fact renders any bias analysis very difficult to perform.

On the other hand, within our simple model, the snowline for Nitrogen (the substance in our list which stays liquid down to the lowest temperature) is placed at 3(2) au from the star in the case of M0(M5) stars. For the same stellar types the tidal locking radius (see below) is approximately 0.3 au, as is seen in the lower panel of Figure 1. Hence the range of interest for our analysis in the case of M stars is smaller than 0.3-3 au. This means that whether the systems are compact (in the sense of lacking planets at large orbital distances) or not, this would not be noticeable at the scales in which we are working.

#### **4 Tidal locking**

When a planet is too close to its star, in the long term tidal locking will happen,

forcing a hemisphere of the planet to be constantly facing the star. The tidal locking radius (Peale 1977, von Bloh *et al.* 2007, Leconte *et al.* 2015) depends on the mass of the star and also on its age, according to:

$$a_{TL} \approx 0.3 t^{1/6} M^{1/3} \quad (4)$$

for  $t$  in gigayears,  $M$  in solar masses and  $a_{TL}$  in au. Gray zones in figure 1 represent the tidal locking regions for three token stellar types. Given the low exponents in equation 4 the tidal locking radius does not change very much among all the types of stars and their possible ages, ranging approximately between 0.1 and 0.4 au.

Tidal locking could make the habitability of a planet very unlikely, as the diurnal hemisphere can reach extremely high temperatures and the nocturnal hemisphere extremely low ones. Although habitability of tidally locked planets cannot be ruled out, in general nothing assures the planetary redistribution of the star energy better than a day-night cycle. In particular, the permanent night side can be an efficient cold-trap for liquids (Leconte *et al.* 2013b, Menou 2013), or destabilize the carbonate-silicate cycle (Kite *et al.* 2011, Edson *et al.* 2012) producing a runaway climate shift by which habitable-zone planets would become uninhabitable, and even cause an atmospheric collapse (Joshi *et al.* 1993, Heng & Kopparla 2013).

On the other hand, several methods have been suggested that could redistribute heat in systems with thick atmospheres and extend the habitable range

through mechanisms that allow atmospheric cycles to transport heat from the dayside to the nightside (Yang *et al.* 2013, Yang *et al.* 2014, Carone *et al.* 2015). Still, these mechanisms are somehow exotic and case-dependent. Besides, another handicap for habitability in worlds very close to a star is the proximity to the possible stellar activity (solar flares or stellar variability), which is specially relevant in the case of red dwarfs (Cohen *et al.* 2014, Williams *et al.* 2015, Kay *et al.* 2016, Airapetian *et al.* 2017).

Therefore, stable oceans and biospheres seem *a priori* much more likely to happen in non-tidally locked worlds that do not need additional mechanisms for heat redistribution. Since the heat transport mechanisms mentioned in the previous paragraph may not be frequent, making it hard to estimate how many planets could benefit of them, we choose to exclude tidally-locked worlds as possible sites for surface seas in our basic model. Nevertheless, there is an additional mechanism which would ensure heat distribution in rocky worlds within the tidally locked radius, whose frequency can be estimated from exoplanetary data. It is the case of rocky satellites orbiting gas giants inside the tidal locking regions (hot Jupiters): in such a case a satellite might not be tidally locked to the star but to its own planet, thus assuring a day-night cycle and an efficient redistribution of stellar energy.

In order to estimate the possible incidence of this last mechanism, we show in Figure 5 (black dots) the total number of planets around stars of a given absolute

magnitude in the exoplanets.org database. Blue dots show the number of those planets that are inside the tidal locking region of their star; interestingly, 83% of planets discovered are inside this zone (which shows a clear observational bias), and red dots are planets inside the tidal locking region that have masses over  $0.36 MJ$ , the lower mass limit to define a hot Jupiter (Winn et al, 2010). Green dots in the inset are the ratio between these two last values, i.e. the fraction of planets inside the tidal locking region that are hot Jupiters for each stellar type. As can be seen, the ratio decreases as the absolute magnitude of stars increase, thus very few hot Jupiters are found around late type stars. The ratio can be modeled by the following exponential (green line in the inset):

$$p \approx 2.25 e^{-0.566M} \quad (5)$$

As hot Jupiters are easier to detect, they are surely over-represented in the data shown in Figure 5, thus this curve represents an upper limit to their real incidence. It may well be that this mechanism is the most frequent for rocky worlds to avoid stellar tidal locking, so in a second approximation we will take equation 5 as a proxy for the probability that a given rocky world in an orbit inside the tidal locking region avoids becoming locked to its parent star. We will measure how such relaxed tidal locking condition changes our results. Afterwards we will consider the effect of an even more relaxed (and less realistic) tidal locking avoidance example.

## 5 Main sequence star numbers in the Galaxy

As Bains (2004) did, the last factor needed in order to estimate the number of planets with possible surface seas is the number density of the different stellar types in our galactic neighborhood, together with their basic properties. We will at least need the stellar surface temperature and radius, which enter the calculation of the surface temperature of a putative planet at a given orbital distance, as well as the stellar mass and age, necessary for the estimation of the tidal locking radius. We will only consider stars along the main sequence for two reasons: they dominate the total numbers, and their properties can be at least approximately encapsulated by simple parameters, as we will show below.

Figure 4 shows the stellar data we have compiled and parameterised for our analysis. We have taken the  $V$ -band absolute magnitude  $M_V$  as the basic classifying parameter, running from  $M_V = -10$  to  $M_V = 20$ , with the solar absolute magnitude being  $M_{V,\odot} = 4.83$ . Although this is not the most usual approach, it allows us to use a continuous variable to monotonically classify stars. To help the reader, the conversion between this scale and the usual OBAFGKM scheme is shown in Figures 4 to 6.

We have taken a number of stars from different types and compiled their temperature, luminosity, mass and radius data from Garrison (1994) and references therein. In Figure 4 those data appear on each panel together with a standard fit or model for each property. The panel at the bottom of Figure 4 shows

the expected maximum main sequence lifetime for each star type (with the current age of the Universe marked as an absolute limit to the stellar age).

The relative abundances of the different stellar types were obtained from LeDrew (2001) and checked with more recent works in Chabrier (2003) and Just *et al.* (2015), and represent the approximate relative abundances of stars of different types in the (extended) solar neighborhood. In this sense, our results will in fact be applicable to the disk of the Galaxy, rather than to the Galaxy as a whole.

## 6 Results and discussion

To estimate the relative abundances of different kinds of seas in the Galaxy disk we take into consideration all the previous inputs: for every type of star, every considered atmospheric pressure, every candidate solvent and different cases of presence or absence of albedo or greenhouse effect, we compute from the melting and boiling points of the substance (Table 1) and from the size and temperature of the star (Figure 4) the corresponding circumstellar habitable zones (Eq. 2). According to our previous result in Section 3, once we have defined the circumstellar habitable regions we calculate the probability to have a planet inside it, assuming a radial probability of presence  $p(a) \propto a^{-1}$ , excluding totally or in part (see below) the region that eventually falls inside the tidal locking radius (Eqs. 4 and 5). The probabilities for every stellar type obtained from this

calculation are then multiplied by the relative type abundances (as given in Figure 4). We repeat this calculation for every considered planetary surface pressure, and finally we calculate their average to obtain our final estimates. The results are shown in Figure 6.

The main left panel shows the average results as a function of the spectral type (top axis) or absolute magnitude (bottom axis) for the case when no albedo or greenhouse is considered and excluding all the planets that fall inside the tidal locking region. We remark that these abundances per spectral type take into account the galactic stock of each stellar type as shown in Figure 4, thus they should not be interpreted as the probability for a star of a given type to have oceans of a given substance, but as an estimation of how many seas of that substance exist in the Galaxy disk around stars of that type. The inset shows the global estimate of galactic relative abundances for seas of each substance to exist on non-tidally locked planets, taking water as reference.

## 6.1 A note about chemistry and mixtures

As we stated in the Introduction we are ignoring the role of photolysis in these results, although it could certainly modulate our conclusions. For example our results predict a high abundance of ammonia seas around Sun-like stars, but we do not find lakes of this substance anywhere in our Solar System. This is due to photolysis by UV solar radiation preventing its long-term stability. The same



effect could be applicable to methane and ethane, where photolysis can reduce the actual abundance of these seas (yet methane and ethane are abundant in Titan, which is still unexplained). Nevertheless ultraviolet radiation is most relevant in early-type stars, which are precisely the least abundant ones; more abundant late types K and M have negligible ultraviolet emission. This is confirmed by *GALEX* measurements (Ortiz and Guerrero, 2016) where far UV emission is measured to fall abruptly for main sequence stars with temperatures under 5000 K, therefore photolysis by UV radiation is not expected to play a relevant role in late-type stars. Note that these late types (see Fig. 6, absolute magnitudes over 6) are the ones dominating the distribution of the most abundant substances: ethane, methane and nitrogen. Note also that these are the colder liquids, thus being farther away from the star and receiving less ionizing radiation. Therefore the relevance of these substances in the frequency of the most abundant exoseas doesn't seem to be dramatically altered by UV photolysis.

Of course all the substances we have studied are not mutually exclusive: the methane melting and boiling points (see Table 1) are practically included in the range of temperatures where ethane is liquid, therefore under the conditions where there is liquid methane, one should expect also liquid ethane (but not necessarily vice versa). In fact in the Solar System we find the satellite of Saturn, Titan, inside both the ethane and methane habitable zones according to Equation 1. The seas found in this world seem to be a mixture of both substances (Lorenz *et al.*

2008, Cordier *et al.* 2012). We have not studied in this work the effect of such and other mixtures, that could potentially change the abundances we obtain. As discussed by Bains (2004), essentially pure liquids like the case of water on Earth may not be the general rule. Thus, these results should not be taken as geochemically realistic but as limit cases. They should, however, be a robust guide for researchers interested in some particular mixture of two of our solvents as long as the chemical properties of the mixture are not widely different from those of the solvents themselves. This seems to be general, as mixtures of substances tend to have thermodynamical properties (including triple and critical point values) that are intermediate between those of the pure components, or at least reasonably close when this is not the case (see for example Conde 2004, Ganesh and Srinivas 2017). Therefore the curve in fig 6 for a mixture of i.e. water and sulfuric acid should show an intermediate behavior of those of pure water and pure sulfuric acid.

## **6.2 Variations on a basic model**

The three right panels show variations with respect to this main reference panel, in the different directions that have been presented in the previous sections.

The top right panel shows the effect in the calculations when we relax the tidal locking exclusion. We allow into our estimate those orbits inside the tidal locking radius that are occupied by giant planets (in a proportion that follows Equation 5),

assuming their rocky moons will be orbitally locked to the parent planet and avoid being locked to the star.

The center and bottom right panels show the effect that is observed when we include an albedo equal to  $A = 0.5$  and no greenhouse effect (center), and a normalized greenhouse effect equal to  $g = 0.5$  and no albedo (bottom). In both cases this parameters are set to all planets, in order to maximise the global effect such a change could induce in the sample.

A remarkable outcome of our study is the high abundance of ethane seas, nine times more probable than water seas, which appear to be found over a wide range of spectral types (practically encompassing the distributions of all the other candidate solvents), and remains stable through the different model variations we analysed. Nitrogen seas also seem to be potentially frequent, specially around red dwarfs. In fact low melting point substances are favored as they remain liquid outside the locking region even for the reddest stars. For instance, had we included molecular Hydrogen as a candidate liquid we would have found  $H_2$  sea abundances about half as frequent as ethane, specially abundant around very late type stars with absolute magnitude over 10. These results are robust and basically independent of the atmospheric pressure considered: ethane seas score systematically highest at every value, followed by nitrogen seas. The same is true when we allow the values of albedo and normalized greenhouse effect to vary within reasonable limits.

### 6.3 Comparison with previous results

The expected relative abundance of different seas that we obtain is coherent with the results in Bains (2004), who obtained also a higher abundance of ethane and nitrogen seas compared to water seas, although to a lesser extent. One of the main reasons for this discrepancy is the introduction of tidal locking as a cut-off that enhances the abundance of low temperature liquids, see for example figure 1 (bottom panel) for the case of the abundant M-type stars, where methane, ethane and nitrogen remain outside the tidal locking region. Nevertheless even when this cut-off is relaxed by not rejecting hot Jupiters, the results are not significantly different: for ethane, the abundance of seas respect to water changes from 9 to 8.3 times, and for nitrogen from 4 to 3.7. This is due to the fact that these substances are prevalent in late-type stars, that seem to lack hot Jupiters in their tidal locking region.

In order to further test the importance of the tidal locking criterium we have performed a second test. We artificially allow a 10% of worlds inside the tidal locking radius to develop an efficient mechanism to transport heat (whichever it may be, taken to be independent of the stellar type as a first approximation). Under this scenario ethane and nitrogen are still the most relevant substances, with ratios respect to water of 4.7 and 2. More dramatically, even in an unrealistic case when the tidal locking has no effect in the inhibition of exoseas, when the

tidal cut-off is completely removed the ratio ethane/water is still high, because the phase space volume available to ethane (yellow region in Figure 2) is larger than that available to water (blue region). Note that in the logarithmic pressure-orbital distance space the shapes and sizes of those regions remain invariant. This fact, combined with the fact that the radial distribution of planets according to a generalized Titius-Bode/Dermott law in logarithmic space becomes a uniform distribution, results in the probability of having a planet inside a given region being directly proportional to the (constant) size of the region in logarithmic space. Thus, in this extreme scenario without any tidal locking cut-off the relative abundances of these liquids become: water 1, ethane 1.84, ammonia 0.64, methane 0.47, nitrogen 0.47, hydrogen sulfide 0.43, hydrogen cyanide 0.37, carbon dioxide 0.1 and sulfuric acid 2.3.

Another remarkable outcome is that, according to our model, most of the habitable worlds with water seas in the Galaxy would orbit stars similar to our Sun. This is a satisfying result from a purely Bayesian point of view: we, being the only case of water-based biology known to ourselves, happen to occupy the most probable niche available to us—a result that was in no way forced into the model. We can also say that, if we ever found alien life *and* it were water-based, most probably the host star of their home planet would be a solar-type star. This may have interesting biological consequences regarding, for example, a common preferred range of the electromagnetic spectrum that our respective visual systems

may share.

Note also that the number of stellar systems harbouring habitable worlds with seas seem to be strongly concentrated in stars with absolute magnitudes roughly in the range 2 to 13, i.e. spectral classes between A0 to M5 approximately. This is due to the fact that beyond M5 (absolute magnitude  $M_V > 13$ ) the habitable zones fall inside the tidal locking region. This also makes our result very little dependent on the details of the (still not very well known) low-mass red dwarf abundances. On the other hand, the low number of seas residing in planets around stars with absolute magnitude  $M_V < 2$  (O and B stars) simply reflects the scarce numbers of such stars in the Galaxy.

## 7 Conclusions

In this work we have expanded upon previous work by Bains (2004), studying the relative cosmic abundance of seas of different solvents taking into account the abundance of every spectral type and the gravitational tidal locking effect. Such abundances are modulated by the radial probability of presence of planets around stars, which we have found is consistent with a universally valid Titius-Bode/Dermott law.

We find that ethane may be the most abundant kind of exosea, eight to ten times more abundant than water, and encompassing planets around a large range of stellar spectral types. Nitrogen seas could also be frequent, especially around

red dwarfs. Water seas seem to be specially localized around Sun-like stars, and their cosmic abundance seems to be relatively low.

Our results suggest that the search for habitable worlds, based on the “follow the water” premise, could be overlooking interesting candidates to habitable planets, albeit for forms of life completely different to our own. Based on these results we could answer our initial question (“Which solvent could be in principle the most frequent for sustaining life?”) stating that, if we were to find life elsewhere in the Universe, their biological machinery would probably be based on ethane.

## **8 Acknowledgements**

The authors want to thank two anonymous referees for their help with an earlier version of this manuscript, and particularly Dr. Chris McKay for a very careful and detailed report, that has greatly contributed to the clarity and reach of our work. We also want to thank Prof. J. Garrido for his valuable help compiling the table of properties of the substances considered in this paper. This work has been funded by projects AYA2013-48623-C2-2 and AYA2016-81065-C2-2 from the Spanish Ministerio de Economía y Competitividad and PrometeoII/2014/060 from the Generalitat Valenciana (Spain).

## **References**

1. Airapetian, V.S., et al., 2017. How Hospitable Are Space Weather Affected

Habitable Zones? The Role of Ion Escape. *The Astrophysical Journal Letters*, 836, L3.

2. Badescu, V., 2010a. Sub-brown dwarfs as seats of life based on non-polar solvents: Thermodynamic restrictions. *Planetary and Space Science*, 58(12), 1650.
3. Badescu, V., 2010b. Tables of Rosseland mean opacities for candidate atmospheres of life hosting free-floating planets. *Central European Journal of Physics*, 8(3), 463.
4. Bains, W., 2004. Many chemistries could be used to build living systems. *Astrobiology* 4(1), 137.
5. Bean, J. et al., 2010. A ground-based transmission spectrum of the super-Earth exoplanet GJ 1214b. *Nature*, 468, 669.
6. Benner, S. A., Ricardo, A. and Carrigan, M. A., 2004. Is there a common chemical model for life in the universe? *Current Opinion in Chemical Biology*, 8, 672.
7. Bleech, M., 2014. Alpha Centauri: Unveiling the Secrets of Our Nearest Stellar Neighbor. In *Astronomer's Universe*. Springer, Netherlands.
8. Bovaird, T., Lineweaver, C.H., 2013. Exoplanet predictions based on the generalized Titius-Bode relation. *Monthly Notices of the Royal Astronomical Society*, 435, 1126.



9. Buchhave, L.A. et al., 2014. Three regimes of extrasolar planet radius inferred from host star metallicities. *Nature*, 509, 593.
10. Carone, L., Keppens, R., Decin, L., 2015. Connecting the dots ? II. Phase changes in the climate dynamics of tidally locked terrestrial exoplanets. *Monthly Notices of the Royal Astronomical Society*, 453(3), 2412.
11. Chabrier, G., 2003. Galactic Stellar and Substellar Initial Mass Function. *Publications of the Astronomical Society of the Pacific* 115, 763.
12. Cohen, O., et al., 2014. Magnetospheric structure and atmospheric joule heating of habitable planets orbiting M-Dwarf stars. *The Astrophysical Journal*, 790, 57.
13. Conde, M., 2004. Thermophysical properties of {NH<sub>3</sub> + H<sub>2</sub>O} solutions for the industrial design of absorption refrigeration equipment. *Engineering*.
14. Cordier, D., et al., 2012. Titan's lakes chemical composition: Sources of uncertainties and variability. *Planetary and Space Science*, 61(1), 99.
15. Dermott, S.F., 1968. On the Origin of Commensurabilities in the Solar System? II The Orbital Period Relation. *Monthly Notices of the Royal Astronomical Society*, 141, 363.
16. Doyle, L.R., 1996. Circumstellar Habitable Zones, *Proceedings of The First International Conference on Circumstellar Habitable Zones*. Edited by Laurance R. Doyle. Menlo Park, CA: Travis House Publications.
17. Edson, A.R., et al., 2012. The carbonate-silicate cycle and CO<sub>2</sub>/climate

- feedbacks on tidally locked terrestrial planets. *Astrobiology* 12, 562.
18. Encrenaz, T., et al., 2005. The Outer Planets and their Moons. *Space Sciences Series of ISSI*, vol 19. Springer, Netherlands.
  19. Ganesh, S., Srinivas, T., 2017. Development of thermo-physical properties of aqua ammonia for Kalina cycle system. *Journal of Materials and Product Technology*, 55, 113.
  20. Garrison, R.F., 1994 in *The MK Process at 50 Years: A Powerful Tool for Astrophysical Insight*. Eds. C.J. Corbally, R.O. Gray and R.F. Garrison.
  21. Gillon, M., et al., 2017. Seven temperate terrestrial planets around the nearby ultracool dwarf star TRAPPIST-1. *Nature* 542, 456.
  22. Goldreich, P., Sciama, D.W., 1965. An Explanation of the Frequent Occurrence of Commensurable Mean Motions in the Solar System. *Monthly Notices of the Royal Astronomical Society*, 130, 159.
  23. Heng, K., Kopparla, P., 2013. On the Stability of Super-Earth Atmospheres. *The Astrophysical Journal*, 754, 60.
  24. Huang, C.X., Bakos, G.A., 2014. Testing the Titius-Bode law predictions for Kepler multiplanet systems. *Monthly Notices of the Royal Astronomical Society*, 442, 674.
  25. Joshi, M.M., Haberle, R.M., Reynolds, T.T., 1993. Simulations of the Atmospheres of Synchronously Rotating Terrestrial Planets Orbiting M Dwarfs: Conditions for Atmospheric Collapse and the Implications for

Habitability. *Icarus* 101, 108.

26. Just, A., et al., 2015. The local stellar luminosity function and mass-to-light ratio in the NIR. *Monthly Notices of the Royal Astronomical Society*, 451 (1), 149.
27. Kasting, J.F., 1988. Runaway and moist greenhouse atmospheres and the evolution of Earth and Venus. *Icarus*, 74(3), 472.
28. Kasting, J.F. et al., 1993. Habitable Zones around Main Sequence Stars. *Icarus*, 101(1), 108.
29. Kay, C., Opher, M., Kornbleuth, M., 2016. Probability of CME impact on exoplanets orbiting M Dwarfs and solar-like stars. *The Astrophysical Journal*, 826, 195.
30. Kite, E.S., Gaidos, E., Manga, M., 2011. Climate Instability on Tidally Locked Exoplanets. *The Astrophysical Journal*, 743, 41.
31. Kopparapu R.K., et al., 2013. Habitable Zones around Main-sequence Stars: New Estimates. *The Astrophysical Journal Letters*, 765, 131.
32. Kopparapu, R.K., 2013. A Revised Estimate of the Occurrence Rate of Terrestrial Planets in the Habitable Zones around Kepler M-dwarfs. *The Astrophysical Journal Letters*, 767, L8.
33. Kotliarov, I., 2008. The Titius-Bode Law Revisited But Not Revived. *physics.space-ph- arXiv:0806.3532*.
34. Lara, P., Poveda, A., Allen, C., 2012. On the structural law of exoplanetary

- systems. *AIP Conference Proceedings* 1479, 2356.
35. LeDrew, G., 2001. The Real Starry Sky. *Journal of the Royal Astronomical Society of Canada*, 95, 32.
  36. Leconte, J., Forget, F., Charnay, B., Wordsworth, R., Pottier, A., 2013a. Increased insolation threshold for runaway greenhouse processes on Earth-like planets. *Nature*, 504, 268.
  37. Leconte, J., et al., 2013b. 3D climate modeling of close-in land planets: Circulation patterns, climate moist bistability, and habitability. *Astronomy and Astrophysics*, 554, A69.
  38. Leconte, J., et al., 2015. Asynchronous rotation of Earth-mass planets in the habitable zone of lower-mass stars. *Science* 347, 632.
  39. Lodders, K., 2003. Solar System Abundances and Condensation Temperatures of the Elements. *The Astrophysical Journal*, 591, 1220.
  40. Lorenz, R.D., et al., 2008. Titan's inventory of organic surface materials. *Geophysical Research Letters*, VOL. 35, L02206.
  41. Lovis, C., et al., 2011. The HARPS search for southern extra-solar planets XXVII. *Astronomy and Astrophysics* 527, A63.
  42. McKay, C.P., Pollack, J.B., Courtin, R., 1991. The greenhouse and antigreenhouse effects on Titan. *Science*, 253(5024), 1118-1121.
  43. Menou, K., 2013. Water-trapped Worlds. *The Astrophysical Journal*, 774, 51.

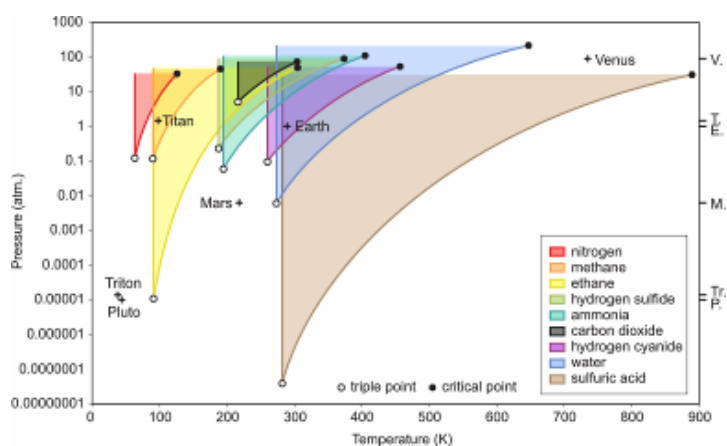
44. NIST Chemistry WebBook, <http://webbook.nist.gov/>
45. National Research Council, The limits of organic life in planetary systems. ISBN 978-0309104845. National Academies Press (2007).
46. Nieto, M.M., 1972. In *The Titius-Bode Law of Planetary Distances: Its History and Theory*. Pergamon Press, Oxford.
47. Ortiz, R., Guerrero, M. A., 2016. Ultraviolet emission from main-sequence companions of AGB stars. *Monthly Notices of the Royal Astronomical Society*, 461(1), 3036.
48. Peale, S.J. 1977, in *Planetary Satellites*, ed. J. A. Burns, 87.
49. Pollack, J.B., 1979. Climatic change on the terrestrial planets. *Icarus*, 37(3), 479.
50. Raval, A., Ramanathan, V., 1989. Observational determination of the greenhouse effect. *Nature* 342, 758.
51. Reynolds, W.C., 1979. *Thermodynamic properties in SI*. Ed. Stanford University. Stanford, CA.
52. Selsis, F., et al., 2007. Habitable planets around the star Gliese 581? *Astronomy and Astrophysics*, 476, 1373.
53. Stevenson, J., Lunine, J. and Clancy, P., Membrane alternatives in worlds without oxygen: creation of an azotosome. *Science Advances* 1, e1400067 (2015).
54. Swain, M. R. et al., 2009. Water, methane, and carbon dioxide present in the

- dayside spectrum of the exoplanet HD 209458b. *The Astrophysical Journal*, 704, 1616.
55. Tinetti, G. et al., 2010. Exploring extrasolar worlds: from gas giants to terrestrial habitable planets. *Faraday Discussions*, 147, 369.
  56. Vladilo, G. et al., 2013. The habitable zone of Earth-like planets with different levels of atmospheric pressure. *The Astrophysical Journal*, 767, 65.
  57. von Bloh, W., et al., 2007. The habitability of super-Earths in Gliese 581. *Astronomy and Astrophysics* 476, 1365.
  58. Williams, P.K.G., et al., 2015. The first millimeter detection of a non-accreting ultracool dwarf. *The Astrophysical Journal*, 815, 64.
  59. Winn, J.N., Fabrycky, D.C., Albrech, S., Johnson, J. A., 2010. Hot stars with hot Jupiters have high obliquities. *The Astrophysical Journal Letters*, 718, L145-L149.
  60. Winn, J.N., Fabrycky, D.C., 2015. The Occurrence and Architecture of Exoplanetary Systems. *Annu. Rev. Astron. Astrophys.*, 53, 409.
  61. Yang, J., Cowan, N.B., Abbot, D.S., 2013. Stabilizing Cloud Feedback Dramatically Expands the Habitable Zone of Tidally Locked Planets. *The Astrophysical Journal*, 771, L45.
  62. Yang, J., et al., 2014. Water trapping on tidally locked terrestrial planets requires special conditions. *The Astrophysical Journal Letters*, 796, L22.
  63. Zsom, A., Seager, S., de Wit, J., Stamenkovic, V., 2013. Toward the

minimum inner edge distance of the habitable zone. *The Astrophysical Journal*,  
778, 109.

**Table 1.** Top: Pressure (atm.) and temperature (K) data for the triple and critical points of the solvents considered in this work. Bottom: Pressure vs. temperature diagram showing the liquid phase for the candidate substances together with the triple and critical points (white and black dots respectively), and the average (P,T) conditions for several rocky worlds in the Solar System. Next to the right margin, the ticks label the surface pressures for those worlds. Data from Reynolds 1979 and the NIST Chemistry WebBook.

Solvent	Triple point		Critical point	
	Pressure (atm.)	Temperature (K)	Pressure (atm.)	Temperature (K)
N <sub>2</sub>	0.1252	63.14	33.987	126.19
CH <sub>4</sub>	0.1169	90.67	46.1	190.6
C <sub>2</sub> H <sub>6</sub>	0.000011	91.6	49.0	305.3
H <sub>2</sub> S	0.232	187.66	89.7	373.3
NH <sub>3</sub>	0.0606	194.95	113	405.4
HCN	0.0968	259.86	53.9	456.7
H <sub>2</sub> O	0.0061	273.17	220.64	647
CO <sub>2</sub>	5.185	216.58	73.8	304.18
H <sub>2</sub> SO <sub>4</sub>	0.000000046	283.0	45.4	927.0





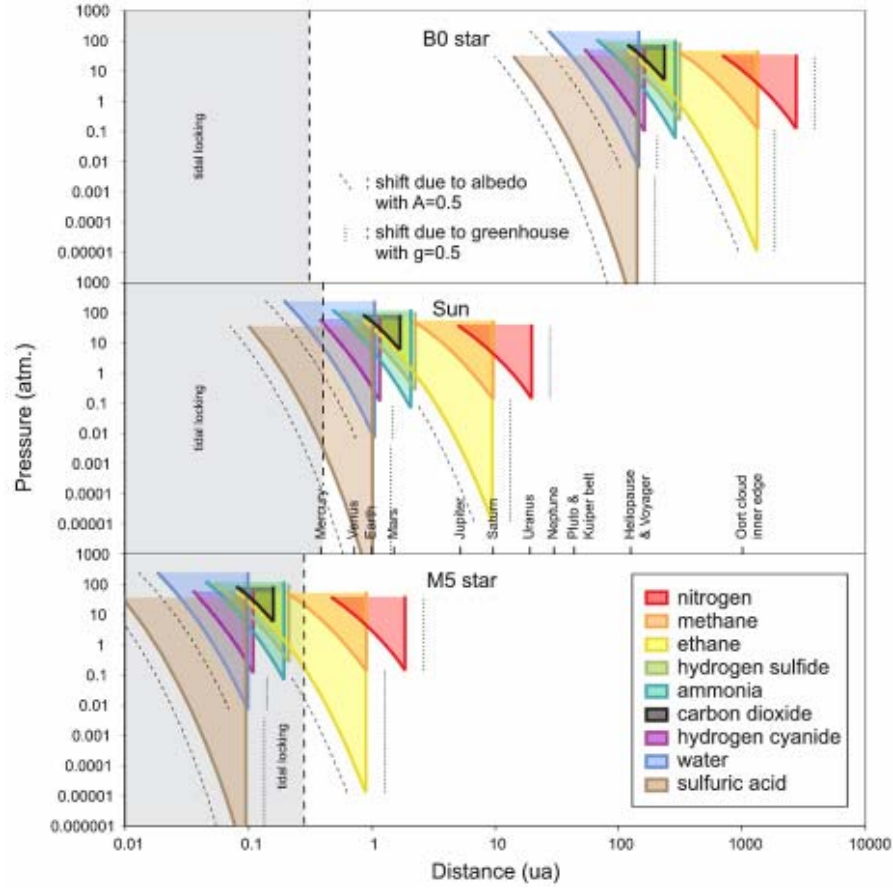


**Figure 1.** Habitable zones as a function of atmospheric pressure and distance to the central star for the nine considered candidate liquids, in the case of a B0 star (top), our Sun (middle) and an M5 star (bottom). Color lines and areas correspond to the simple model that includes no albedo or greenhouse effect. Dashed black lines represent the shift they suffer considering an albedo of  $A=0.5$  (and no greenhouse effect); dotted black lines represent the shift due to an normalized greenhouse of  $g=0.5$  (and 0 albedo). The gray zones correspond to the regions affected by tidal locking.

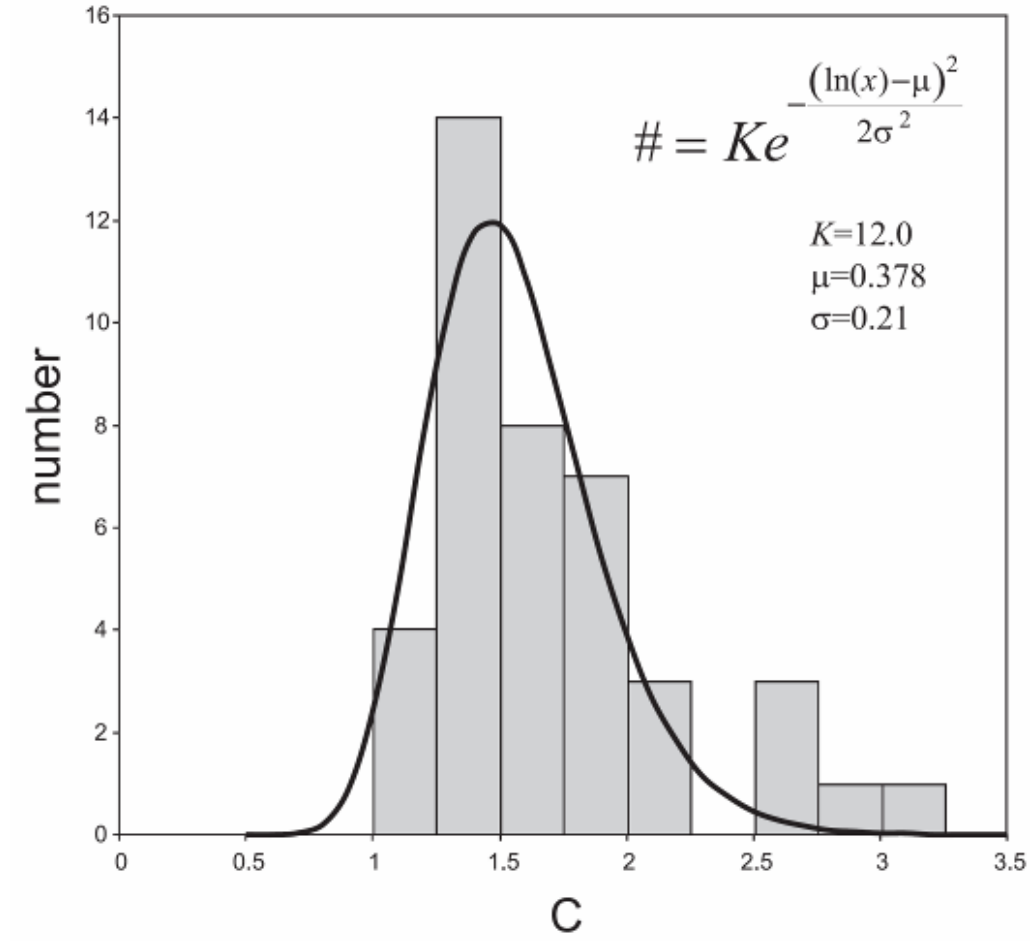


**Figure 2.** Histogram of the growth factor  $C$  (see equation 3) for the Titius-Bode/Dermott’s law extracted from Lovis *et al.* (2011), Lara *et al.* (2012), Bovaird & Lineweaver (2013), Huang & Bakos (2014), and Gillon *et al.* (2017), together with a fit to a lognormal function.

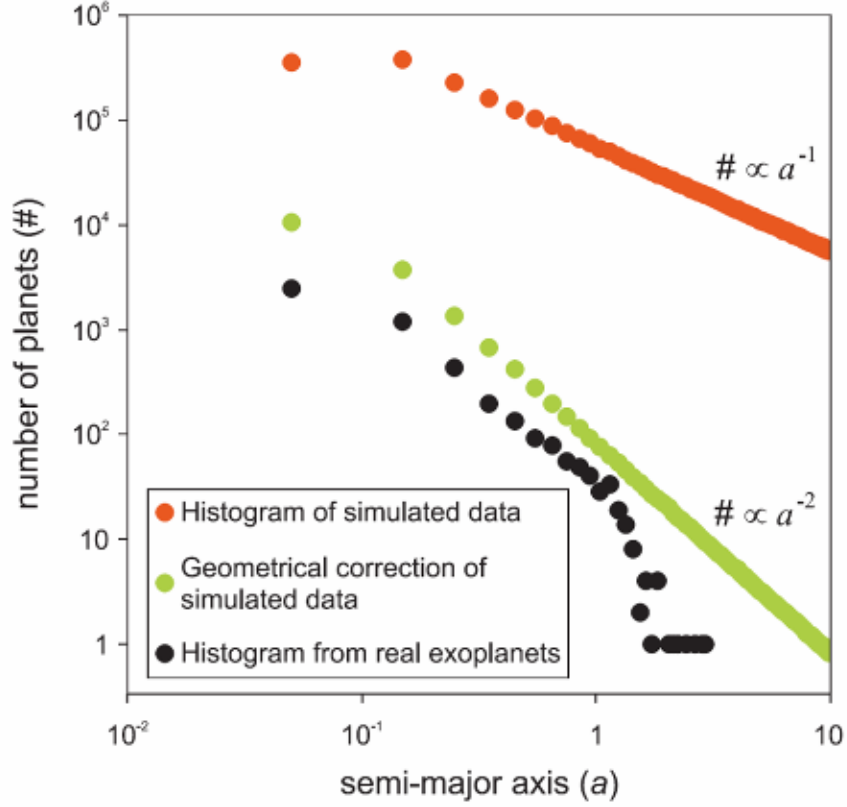


**Figure 3.** Histograms of orbital semi-major axis: Red dots: histogram for 100,000 computer-simulated planetary systems following the Titius-Bode/Dermott’s law. Green dots: histogram for the fraction of planets from the previous simulation which are expected to be observable by the transit method. Black dots: histogram for truly detected exoplanets by the transit method extracted from Exoplanets Data Explorer ([exoplanets.org](http://exoplanets.org)). In all the cases the binning scale of the histograms is 0.1 au. The main discrepancy arises for distances higher than 1 au, and can be explained by the fact that they imply orbital periods of several years, an additional bias that hinders observations.

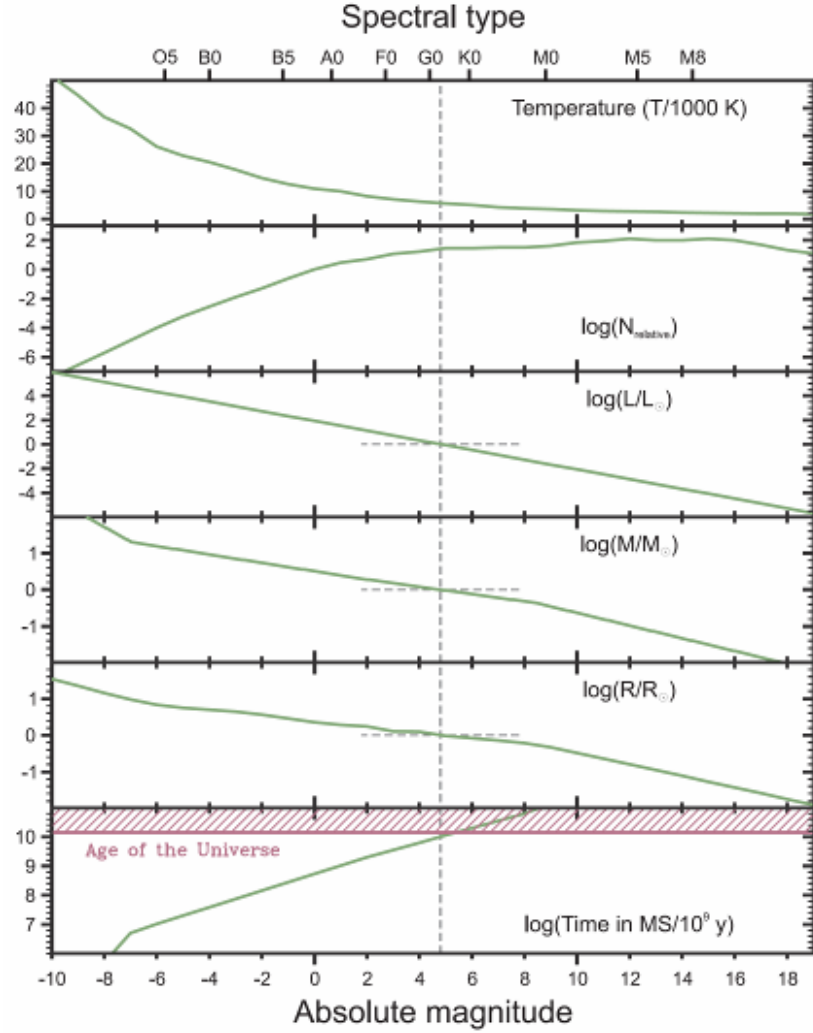


**Figure 4.** Surface temperature, relative abundance, luminosity, mass, radius and maximum main sequence age for stars of different absolute magnitude ranging from  $M_V = -10$  to  $M_V = 20$ . The absolute magnitude of the Sun is marked with a vertical line, and the solar luminosity, mass and radius are also marked with horizontal lines in their respective panels. The positions of some stellar type standards are marked along the top margin as reference.

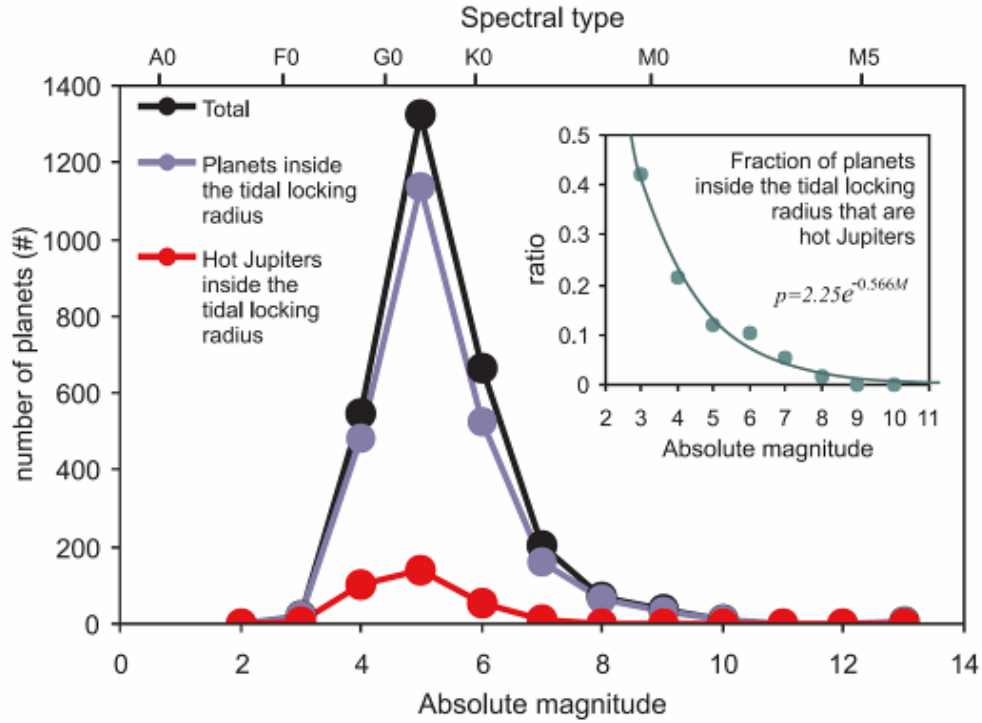


**Figure 5.** Frequency of hot Jupiters inside the tidal locking region as a function of the spectral type/absolute magnitude. Main panel shows the total number of planets found around each type of star (black dots), the number of those planets that are inside the tidal locking region (blue dots) and the number of planets inside this region that are hot Jupiters (red dots). The inset shows the ratio between these two last numbers together with an exponential fit.

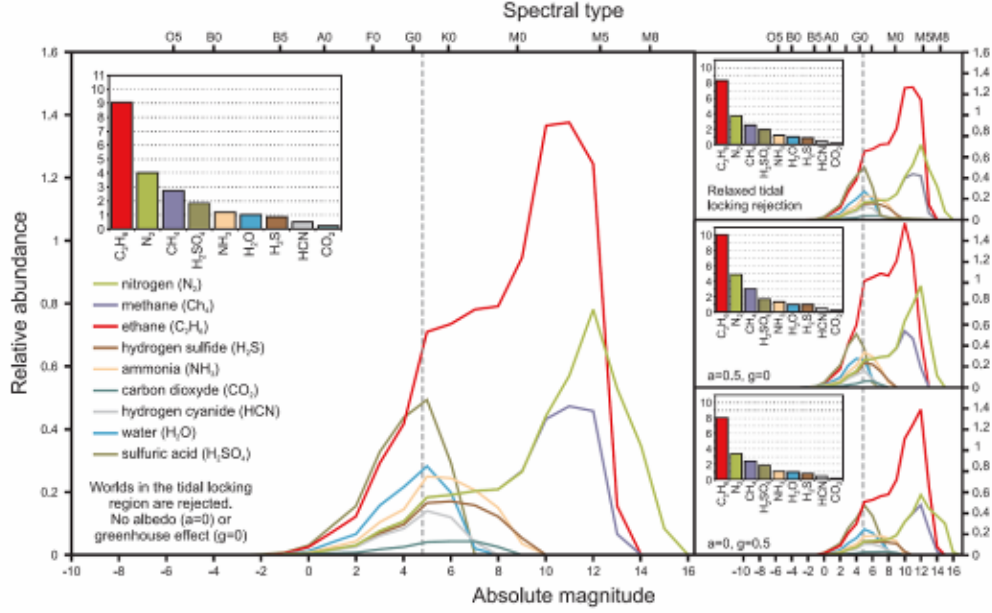


**Figure 6.** Estimated relative abundances of seas in the Universe for different candidate solvents as a function of the stellar type/absolute magnitude. The main panel shows the average result, assuming no albedo or greenhouse effect and rejecting all the planets inside the tidal locking radius, with the histogram inset showing the integral of such average (normalized to 1.0 for the case of water, which is taken as the reference value). The vertical dotted line marks the spectral type of the Sun. For comparison, the right top panel shows the effect of relaxing tidal locking rejection by including hot Jupiters inside the tidal locking radius; the right center panel displays the effect of assuming an albedo of  $A = 0.5$  and no greenhouse effect ( $g = 0$ ); and the right bottom panel displays the case of a greenhouse effect of  $g = 0.5$  and no albedo ( $A = 0$ ).